Experimental and analytical evaluation of the response time of high temperature fiber optic sensors

Paula Rinaudo[1*], Ignacio Paya-Zaforteza[1], Pedro A. Calderón[1], Salvador Sales[2]

[1]*ICITECH, Departamento de Ingeniería de la Construcción y Proyectos de Ingeniería Civil, Universitat Politècnica de València, Camino de Vera s/n, 46022, Valencia, Spain.*

[2] *ITEAM, Departamento de Comunicaciones, Universitat Politècnica de València, Camino de Vera s/n, 46022, Valencia,Spain.*

Authors e-mail addresses:	Paula Rinaudo:	pauri@posgrado.upv.es
	Ignacio Paya-Zaforteza:	igpaza@cst.upv.es
	Pedro A. Calderon:	pcaldero@cst.upv.es
	Salvador Sales Maicas:	ssales@dcom.upv.es

Abstract

Gas temperature is a key variable in many high temperature applications. Sensors for measuring gas temperatures must be selected according to many different criteria, response time being one of the most important. Response time quantifies the time that the sensor needs to react to a sudden temperature variation. When rapid temperature fluctuations are expected, as in the case of fire tests, significant instantaneous errors can occur if the sensor response time is longer than the duration of the temperature fluctuation. Despite the importance of response time, there is no general agreement on how to quantify this value in high temperature fiber optic sensors.

This paper proposes a methodology to estimate the response time of fiber optic temperature sensors based on an analytical model of the heat transfer between the sensor and its surroundings. The method is validated by an experimental study. In addition, the response times of three different high temperature fiber optic sensors developed by the authors are compared with each other and with the response time of some widely used thermocouples. The results show i) that fiber optic sensors have a significantly shorter response time than thermocouples with similar packaging, ii) that the response time is shorter during the heating phase than the cooling phase, and iii) highlight the importance of considering this parameter in the sensor selection process.

Keywords: Response time, fast high temperature sensors, sensor selection, RFBG

* Corresponding author.

Experimental and analytical evaluation of the response time of high temperature fiber optic sensors

Paula Rinaudo, Ignacio Payá-Zaforteza, Pedro Calderón, Salvador Sales

Highlights:

- A new method is developed to estimate response times of FO temperature sensors
- Factors that influence the response time are discussed
- Fiber optic sensors can have significantly smaller response time than thermocouples

Abstract

Gas temperature is a key variable in many high temperature applications. Sensors for measuring gas temperatures must be selected according to many different criteria, response time being one of the most important. Response time quantifies the time that the sensor needs to react to a sudden temperature variation. When rapid temperature fluctuations are expected, as in the case of fire tests, significant instantaneous errors can occur if the sensor response time is longer than the duration of the temperature fluctuation. Despite the importance of response time, there is no general agreement on how to quantify this value in high temperature fiber optic sensors.

This paper proposes a methodology to estimate the response time of fiber optic temperature sensors based on an analytical model of the heat transfer between the sensor and its surroundings. The method is validated by an experimental study. In addition, the response times of three different high temperature fiber optic sensors developed by the authors are compared with each other and with the response time of some widely used thermocouples. The results show i) that fiber optic sensors have a significantly shorter response time than thermocouples with similar packaging, ii) that the response time is shorter during the heating phase than the cooling phase, and iii) highlight the importance of considering this parameter in the sensor selection process.

Keywords: Response time, fast high temperature sensors, sensor selection, RFBG

1. Introduction

The importance of measuring gas temperatures in certain industrial applications for infrastructure monitoring or in laboratory fire tests, has motivated a lot of research on high temperature sensors (e.g. [1-4]). This line of research is challenging, not least because temperature sensors indicate their own temperature (Moffat, 1962), so that even when the gas temperature is constant, a transient heat transfer takes place through the sensor until it reaches the temperature of the surrounding gas.

The time the sensor needs to reach a certain percentage of the temperature of the surrounding gas is called its response time. The importance of response time has been shown by several studies focused on the measurement of this parameter (see e.g. [5-8]). Research has also been carried out [9] that shows that selecting the appropriate sensor by its response time is crucial, in order to avoid significant instantaneous errors, especially in applications in which large gas temperature fluctuations occur on time scales shorter than the response time. For example, Figure 1 shows the temperature measurements of two thermocouples with different diameter during a gas fire test [9]. It can be seen that the response time of the thermocouple with higher diameter is larger than the fluctuation of the gas temperature and as a consequence the measurement error is significant. In this example the maximum error is close to 200ºC.

Surprisingly, despite the importance of response time and the errors that it can induce, there is no common agreement on how to evaluate it. Yeo et al. [5] quantify it as the time that the sensor needs to reach 90% of the variation of the surrounding gas temperature. Other authors, such as Barrera et al. [6] define it as the time required for the sensor to rise from 10% to 90% of the final temperature of the surrounding gas, and still others (e.g. [7,8]) as the time needed by the sensor to achieve 63.2% of the surrounding gas temperature variation. Some commercial thermocouple manufacturers provide information about the response time of their thermocouples. For example, RDC Control [10] gives the thermocouple response time for a temperature increase of 80°C and Watlow [11] provides the average response time in the heating phase. However, the procedure used to obtain this time is not always described in the thermocouple specifications. Furthermore, it is usually defined for thermocouples only in the heating phase and not the cooling phase, so that the discrepancy in criteria makes it difficult to compare the response time of different sensors.

Within this context, this paper proposes a methodology to evaluate the response time of high temperature fiber optic sensors and applies it to estimate the response time of three different high temperature fiber optic sensors developed by the authors. The methodology is an improvement on the EGOLF recommendations [8] for the use of thermocouples in fire tests and is based on analytical and experimental studies. Section 2 of the paper details the basics of heat transfer between the gas and the sensor and the concept of response time. Section 3 describes the analytical and experimental methodology used in the study to evaluate response time. Section 4 compares the response time of the fiber optic sensors obtained from the analytical model and the experimental methodology. This section also compares the response time of thermocouples and fiber optic sensors. Section 5 details the main conclusions of this work.

2. Dynamic response of a temperature sensor

The response time of a system is the description of the output response of the system as a function of time when the system is subjected to an input. The response of a system submitted to a temperature change is characterized by the transient response and the steady state response. The former is the response of the system from the time at which the input is applied until the time when the output reaches the steady state. The latter is the phase when the output reaches the input value [12].

The response of a temperature sensor can be expressed as an energy balance between the rate of change of the internal energy of the sensor and the rate of heat transfer between the sensor and the surrounding gas temperature [13] as shown in Equation 1.

$$\mathrm{m.c_p.dT = h.A.(T_{gas}\text{-}T_{sensor})dt} \qquad (1)$$

Where *m* is the mass of the sensor obtained by the product of its density (ρ) and its volume (V); c_p is the specific heat of the sensor; *h* is the net heat transfer coefficient between the sensor and the surrounding gas; *A* is the exposed surface area of the sensor; T_{gas} is the gas temperature and T_{sensor} is the temperature recorded by the temperature sensor. This equation can be rewritten as:

$$T_{gas} = T_{sensor} + \frac{\rho.V.c_p}{h.A}.\frac{dT}{dt} \quad (2)$$

Under the hypothesis that the sensor has uniform temperature along its body and through its cross section, the response of a temperature sensor can be modeled as a first order system as shown in Equation 3 [14,15].

$$T_{gas} = T_{sensor} + \tau \frac{dT}{dt} \quad (3)$$

Where τ is a coefficient called *time constant* which from Equation 1 and Equation 3 can be defined as:

$$\tau = \frac{\rho.V.c_p}{h.A} \quad (4)$$

Thus, the time constant depends on several properties of both the sensor itself and the operating conditions. It is important to highlight that the heat transfer coefficient between the sensor and the surrounding gas, *h*, is a key factor and is influenced by numerous factors, such as the velocity and the temperature of the fluid in which the sensor is immersed [16]. Therefore τ is not a constant value and it is important to indicate the boundary conditions used to obtain it.

3. Evaluation of response time

According to EGOLF [8] the response time of a thermocouple is the time that the thermocouple needs in still air to respond to a step change in its surrounding gas temperature from an initial value T_0 to a final value T_f (see Fig. 2). Response time is evaluated experimentally as the time taken by the thermocouple to achieve 63.2% of the difference between T_0 and T_f. This definition is based on the study of the response of the sensor to a nearly instantaneous change in its surrounding gas temperature from T_0 to T_f. In this case, Equation 3 can be solved (see e.g. [17]) and the temperature of the sensor as a function of time can be expressed as:

$$T_{sensor}(t) = T_f + (T_0 - T_f)e^{-\frac{t}{\tau}} \quad (5)$$

In this equation, when time is equal to the time constant (t=τ), the temperature in the sensor is equal to 63.2% of the total temperature change. Thus, the time constant corresponds to the response time, as can be seen in Figure 2.

EGOLF guidelines recommend evaluating response time by inserting the sensor into a preheated furnace and to remove it immediately when the temperature stabilizes. The furnace temperature at the start of the test should be 700°C and the response time should be obtained during the cooling phase. However, different thermocouple manufacturers (for example [10]) usually evaluate it in the heating phase by subjecting the thermocouple to a step change from ambient temperature to 100°C.

To evaluate the response time of high temperature fiber optic sensors and to compare the results with those of thermocouples, the response time is calculated in this study for both heating and cooling phases using an approach which is a hybrid of the EGOLF and manufacture methods. It is first evaluated experimentally, considering four temperature variations and then the experimental results are used to calibrate an analytical model. Finally, the analytical model is used to obtain the response time for other temperature variations.

3.1. Experimental evaluation of response time

Three fiber optic sensors (FOS) and two type-k thermocouples (TC) were subjected to tests. The FOS were developed by the authors [18] and are based on Regenerated Fiber Bragg Grattings (RFBGs) to withstand temperatures up to 1200ºC. RFBGs are fiber Bragg gratings that undergo a physical and chemical process to be able to resist high temperatures. To create the RFBGs the fiber is first placed into a hydrogenation chamber at room temperature. Then, the FBG is inscribed into the hydrogen loaded fiber using a laser and finally, the RFBGs are regenerated in a subsequent annealing process. To create these RFBGs and the sensors based on this technology, standard telecommunication optical fibers and RFBGs with a grating length equal to 0.5 cm were used. The sensors had tubular packaging of three different types: two were metallic (henceforth FOS A and FOS C) and one ceramic (FOS B). FOS A packaging external diameter was 1.5mm and its thickness was 0.15mm. The external diameter and thickness of FOS B and FOS C packaging was 2mm and 0.5mm respectively. One of the thermocouples tested (henceforth TC A) was a shielded ungrounded thermocouple with a probe of 250 mm length and similar packaging characteristics to FOS A (diameter 1.5 mm). The other was a bare bead thermocouple with isolated ceramic fiber cable (2 x 0.8mm) commonly used in fire tests (henceforth TC D). Note that the sensors were named following the criteria that each letter represents a type of packaging, then FOS A and TC A have the same packaging and FOS B, FOS C and TC D have all different packaging conditions.

A tubular Carbolite MTF 12/38/48 furnace was used for the response time test at four different temperatures, T_f (100, 200, 300 and 400 °C).The response time of each sensor was evaluated first in the heating phase, τ_h, from initial temperature, T_0, to furnace temperature, T_f, and then in the cooling phase, τ_c, from furnace temperature to ambient temperature, T_a. Figure 3 shows the experimental set up (furnace, furnace opening, fiber optic sensor, thermocouple and interrogator).

The furnace was heated to the specified furnace temperature and then stabilized. The sensor was rapidly placed inside the furnace through a small opening in the shortest possible time. When the sensor reached a stable temperature, it was quickly removed from the furnace and maintained at ambient temperature at least 10 cm away from any surface. It was found that both, the shortest possible time to place the sensor inside the furnace and the time to quickly removed, was one second. This time is called Δ on the analytical evaluation of the response time.

The sensors response was recorded every second throughout the test using a Micron Optics sm125-500 optical sensing interrogator for the fiber optic sensors and a Eurotherm 3216 thermocouple controller for the thermocouples. Figure 4 shows a typical sensor response.

3.2. Analytical evaluation of response time

The response time of the fiber optic sensors was analyzed twice. First, a simplified zero-dimensional model was solved through simple equations. Then a non-linear heat transfer model was developed with Abaqus software [19]. The results of the models showed that the simplified model hypothesis was acceptable and provided accurate results. The coefficients involved in the models were calibrated with the results obtained in the experimental tests.

The simplified model solves Equation 6, which is obtained from Equation 2, for each sensor in incremental time steps,

$$T_{sensor} = T_{gas} - \frac{\rho.V.c_p}{h.A}.\frac{dT}{dt} \quad (6)$$

Solving Equation 6 requires the definition of:

- The gas temperature function T_{gas} which describes the temperature in the gas around the sensor as a function of time. This function is given by Equation 7.

$$\begin{cases} t \leq 0 & T_{gas}(t) = T_0 \\ 0 < t < \Delta & T_{gas}(t) = T_0 + \frac{(T_f - T_0)}{\Delta}\, t \\ t \geq \Delta & T_{gas}(t) = T_f \end{cases} \quad (7)$$

Where Δ is the time taken to place the sensor inside the furnace and T_0 and T_f are as defined above. After some iterations value Δ was defined as 1 second. It is very important to keep this value constant in order to get repetitive results. Since a variation of the time taken to place and/or remove the sensor into/from the furnace modifies the gas temperature function and as a consequence, the response of the sensor.

- The material properties (tube wall thickness *e*, density ρ and specific heat c_p) of each sensor. Initial values of these parameters were taken from the material technical data specifications and were calibrated with the experimental results.

- The net heat transfer coefficient between the sensor and the surrounding gas, $\dot{h}$. This coefficient is defined as the sum of the net radiative flux, $\dot{h}_{net,r}$, and the net convective flux, $\dot{h}_{net,c}$, as follows (see e.g. [20]):

$$\dot{h} = \dot{h}_{net,r} + \dot{h}_{net,c} = \varepsilon . \kappa . \left[\left(T_{gas} + 273\right)^4 - \left(T_{sensor} + 273\right)^4 \right] + \alpha_c \left(T_{gas} - T_{sensor}\right) \quad (8)$$

Where ε is the emissivity, which varies with the material; κ =5.67 x10^{-8} W/(m^2 K^4) is Stefan-Boltzman constant and α_c is the convective heat transfer coefficient. The convective heat transfer coefficient and the emissivity of the exposed surface were calibrated from the experimental results for both the cooling and heating phase. The convective heat transfer coefficient resulted to be 70 W/(m^2 K) for the heating phase and 35 W/(m^2 K) for the cooling phase. The emissivity was 0.4 for FOS A, 0.7 for FOS B and 0.8 for FOS C.

Then, the temperature increment of the sensor for each time step can be obtained as:

$$\Delta T_{sensor} = \frac{A}{\rho . V . c_p} \Delta t \left(\varepsilon . \kappa . \left[\left(T_{gas} + 273\right)^4 - \left(T_{sensor} + 273\right)^4 \right] + \alpha_c \left(T_{gas} - T_{sensor}\right)\right) \quad (9)$$

And, finally, the sensor temperature for each time interval can be calculated as:

$$T_{sensor}(t + \Delta t) = T_{sensor}(t) + \Delta T_{sensor} \quad (10)$$

The main hypothesis of this simplified model is that temperature is uniform throughout the sensor. To verify that this hypothesis is acceptable, a non-linear heat transfer model was developed with the finite element analysis software Abaqus [19]. Each sensor was modeled as a hollow cylinder with a length of 10 cm. The internal and external diameters were defined for each sensor according to its dimensions (Figure 5a). The finite element model also assumed that the heat is transferred immediately from the internal surface of the packaging to the fiber. Therefore, neither the fiber nor the air between the packaging and the fiber were modeled. Abaqus element DC3D8 for heat transfer elements were used to mesh the hollow cylinder consisting of a three dimensional eight-node linear heat transfer solid element with one degree of freedom per node. The section of the cylinder was meshed regularly with 10 divisions along the thickness and 80 along the diameter as shown in Figure 5b.

Since each sensor packaging was of a different material, the thermal properties and density were defined in each case in accordance with the material provider's specifications.

Thermal loads were applied in two steps. The first step defined an initial temperature condition of the sensor specimen equal to T_0. In the second step the thermal loads were applied following the function defined as gas temperature (from T_0 to T_f). Surface film condition and surface radiation interactions were applied to the external surface of the cylinder (exposed surface).

Figure 6 shows an example of the results obtained from the non-linear heat transfer model and gives the temperature along the cross section of the fiber optic type A sensor for a furnace temperature of 100°C after an 8-second simulation. It can be observed that the external surface of the cylinder has a temperature of 71.955°C while the internal is at 71.947°C. The maximum temperature variation along the sensor cross section is 0.011%, so that temperature can be considered to be uniform within it. Similar results were obtained for all the sensors and temperature ranges considered. Consequently, the hypothesis that the temperature is uniform within the cross section can be accepted.

4. Results

4.1 Response time of the Fiber Optic Sensors

This section gives the results of the experimental tests and the calibrated analytical simulation of the response time. Experimental evaluation was done up to 400°C and enabled the validation of the analytical model explained in Section 3.2. The analytical model was then used to obtain the response time of the fiber optic sensors up to the maximum temperature they are able to measure.

Figures 7, 8 and 9 show the response for the heating and cooling phase for the three fiber optic sensors: FOS A, FOS B and FOS C. In each of these phases the experimental tests were conducted at four furnace temperatures (100, 200, 300 and 400°C). Temperatures were plotted using a gray scale, where the lighter gray represents the higher temperature and the darker gray the lower. Each temperature is represented by the same gray in all the figures. The experimental responses of the fiber optic sensors are plotted with circles and the analytical solutions in continuous lines. A dashed horizontal line is plotted for each furnace temperature and represents the temperature at which the response time is defined. This is $T_0+0.632\ (T_f-T_0)$ for the heating phase and $T_f+0.632\ (T_a-T_f)$ for the cooling phase. The response time of a sensor for a given furnace temperature can be obtained graphically from the intersection of the sensor response and the dashed line.

After validating the analytical solution, the response times of the fiber optic sensors were calculated for furnace temperatures from 100°C up to the maximum temperature of each sensor. Table 1 gives the results.

As expected, the results show that FOS A is much faster than FOS B and C because its packaging is significantly thinner. FOS B and C, with the same packaging geometry, have different response times, due to their different material properties. The response times obtained are not constant and vary with temperature. The maximum response times were obtained with furnace temperature equal to 100°C (minimum temperature).

The response time variation with temperature increases with the thickness of the sensor packaging. The sensors studied had a faster response during the heating phase than the cooling phase.

It is important to highlight that each sensor type was submitted to several heating-cooling cycles for each temperature and no hysteresis was appreciated.

4.2. Response time of thermocouples and comparison with fiber optics sensors

Figure 10 shows the results of the experimental tests on TC A, whose packaging properties and dimensions are very similar to FOS A. To facilitate comparison, the FOS A experimental results are also plotted by circles and TC A results by an “x”.

The experimental results of the TC D response time tests are given in Figure 11.The experimental FOS A results are also plotted as a reference. FOS A results are shown in circles and TC D in squares.

Table 2 summarizes the TC A, TC D and FOS A response times for both heating and cooling phases and for four furnace temperatures.

FOS A can be seen to have a faster response than TC A and TC D in both heating and cooling phases. For example, the TC A response time obtained at a furnace temperature of 100°C during the heating phase was 13.0s, and for TC D was 24.0s, while FOS A shows a response time of 8.3s under the same conditions. This means that for sensors with similar packaging (FOS A and TC A) FOS has a 57% faster response. Two facts explain this difference. First of all, the packaging of FOS A consists of a hollow tube containing only the fiber optic inside, whereas the hollow tube of TC A is not empty. Secondly, the diameter of the fiber optic is significantly smaller than the diameter of the thermocouple wires. In the cooling phase, FOS A had a response time of 15.4s, TC A 24.0s and TC D 37.1s. FOS A was thus 56 % faster than TC A and 141% faster than TC

D in this phase. Similar results were obtained for the other furnace temperatures studied. The results clearly show that TC D has a much slower dynamic response than FOS A.

5. Conclusions

Response time is a vital parameter when selecting a temperature sensor, as underestimating it can lead to significant measurement errors. However, despite its importance, to date there has not been any generally accepted method of obtaining the response time of fiber optic temperature sensors. This paper proposes a method of estimating the response time of high temperature fiber optic sensors. This method was evaluated by both, an analytical model based on the heat transfer between the temperature sensors and the surrounding environment and an experimental study. The response times of three different high temperature fiber optic sensors developed by the authors were also compared with each other and (in the case of FOS A) with the response time of commonly used thermocouples. The results obtained show that:

- The analytical model applied in this paper can successfully be used to predict the response time of fiber optic sensors.
- Response time depends on: whether the sensor is heated or cooled, the range of the temperature change, the thermal properties of the sensor packaging and the properties of the surrounding environment.
- The thinner the packaging of the fiber optic sensor, the smaller the response time.
- Response time is shorter during the heating phase than the cooling phase.
- Although FOS A and TC A had similar packaging characteristics, FOS A has a shorter response time than TC A. This difference is variable and can be up to 57%, which is an important advantage of the fiber optic sensor.

Acknowledgments

This work has been possible thanks to the financial support of the Spanish Ministry of Science and Innovation (Research Project BIA 2011-27104). Funding for this research has been provided to Paula Rinaudo by the European Commission (Erasmus Mundus Action 2 ARCOIRIS).

Bibliography

[1] R. Zhao, G. Shao, Y. Cao, L. An, C. Xu, Temperature sensor made of polymer-derived ceramics for high-temperature applications, Sensors Actuators A Phys. 219 (2014) 58–64. doi:10.1016/j.sna.2014.08.012.

[2] C. Huang, D. Lee, J. Dai, W. Xie, M. Yang, Fabrication of high-temperature temperature sensor based on dielectric multilayer film on Sapphire fiber tip, Sensors Actuators A Phys. 232 (2015) 99–102. doi:10.1016/j.sna.2015.05.017.

[3] P. Rinaudo, B. Torres Górriz, D. Barrera Villar, I. Payá Zaforteza, P. Calderon Garcia, S. Sales Maicas, Application of fiber optic high temperature sensors for structural monitoring of structures submitted to fire, IABSE Symp. Rep. 102 (2014) 2932–2938. doi:10.2749/222137814814069598.

[4] W. Wu, X. Liu, Investigation on High Temperature Characteristics of FBG Sensors, Opt. - Int. J. Light Electron Opt. 126 (2015) 2411–2413. doi:10.1016/j.ijleo.2015.06.009.

[5] T.L. Yeo, T. Sun, K.T. V Grattan, D. Parry, R. Lade, B.D. Powell, Characterisation of a polymer-coated fibre Bragg grating sensor for relative humidity sensing, Sensors Actuators, B Chem. 110 (2005) 148–156. doi:10.1016/j.snb.2005.01.033.

[6] D. Barrera, V. Finazzi, J. Villatoro, S. Sales, V. Pruneri, Packaged Optical Sensors Based on Regenerated Fiber Bragg Gratings for High Temperature Applications, 12 (2012) 107–112.

[7] D. Zhang, J. Wang, Y. Wang, X. Dai, A fast response temperature sensor based on fiber Bragg grating, Meas. Sci. Technol. 25 (2014) 075105. doi:10.1088/0957-0233/25/7/075105.

[8] EGOLF (European group of organizations for fire testing, inspection and certification) 2008, EGOLF Agreement EA 01 : 2008, Determination of the response time of thermocouples to be used for the measurement of air or gas phase temperature in reaction to fire testing, (2008) 1–8.

[9] W. Pitts, Temperature Measurements in Fires. Measurement Needs for Fire Safety: Proceedings of an International Workshop, National Institute of Standards and Technology (2000).

[10] RDC Control, Thermocouple Response time, www.rdccontrol.com (accessed July 12, 2015).

[11] Watlow, Thermocouples. General Information, www.watlow.com (accessed July 3, 2015).

[12] S.K. Gupta, *Elements of control system,* Prentice Hall PTR, 2001.

[13] A.F. Mills, *Basic heat and mass transfer*, Pearson College Div, 1999.

[14] A. Terzis, J. Von Wolfersdorf, B. Weigand, P. Ott, Thermocouple thermal inertia effects on impingement heat transfer experiments using the transient liquid crystal technique, 11 (2012). doi:10.1088/0957-0233/23/11/115303.

[15] W. Pitts, E. Braun, R. Peacock, H.E. Mitler, E. L. Johnson, P. A. Reneke, L. G. Blevins, Temperature uncertainties for bare-bead and aspirated thermocouple measurements in fire environments, *ASTM Special Technical Publication* 1427 (2003): 3-15.

[16] M. Tagawa, Y. Ohta, Two-thermocouple probe for fluctuating temperature measurement in combustion - Rational estimation of mean and fluctuating time constants, Combust. Flame. 109 (1997) 549–560. doi:10.1016/S0010-2180(97)00044-8.

[17] D.E. Seborg, D.A. Mellichamp, T.F. Edgar, F.J. Doyle, *Process dynamics and control, third edition,* John Wiley & Sons, 2010.

[18] P. Rinaudo, B. Torres, I. Paya-Zaforteza, P.A. Calderón, S. Sales, Evaluation of new regenerated fiber Bragg grating high-temperature sensors in an ISO 834 fire test, Fire Saf. J. 71 (2015) 332–339. doi:10.1016/j.firesaf.2014.11.024.

[19] Simulia, Abaqus 6.13

[20] T.L. Bergman, E.P. Incropera, A.S Lavine, Fundamentals of heat and mass transfer, John Wiley & Sons, 2011.

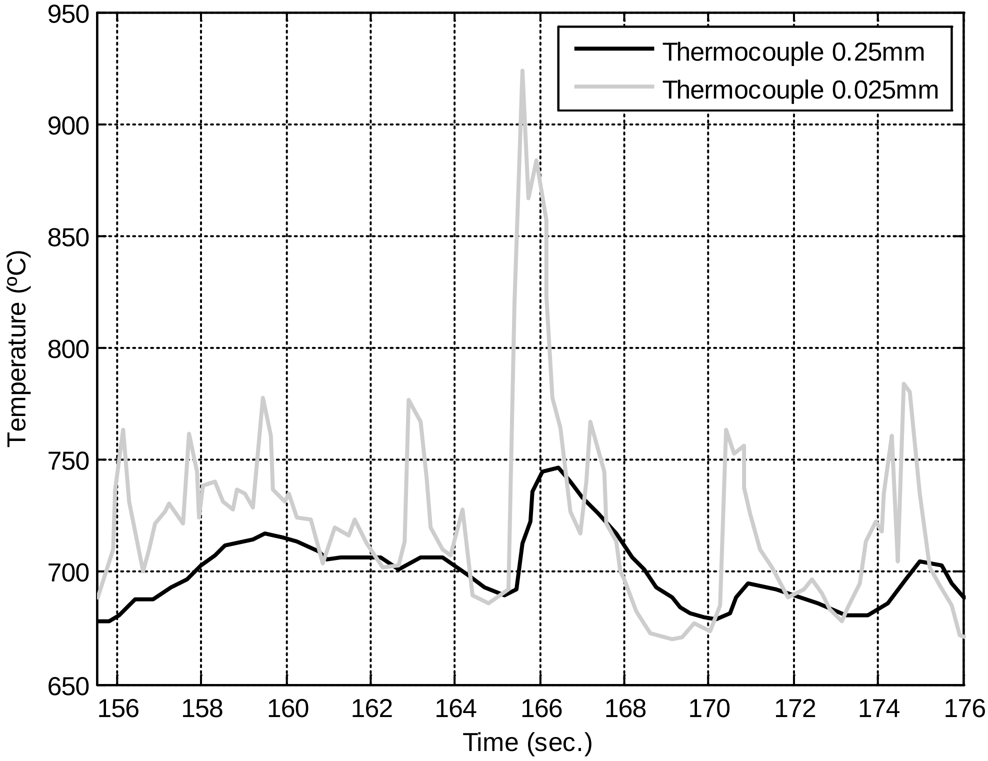

Figure 1 Temperature measured during a gas fire test [9] by a thermocouple with a diameter of 0.25mm (black line) and a thermocouple with a diameter of 0.025mm (gray line).

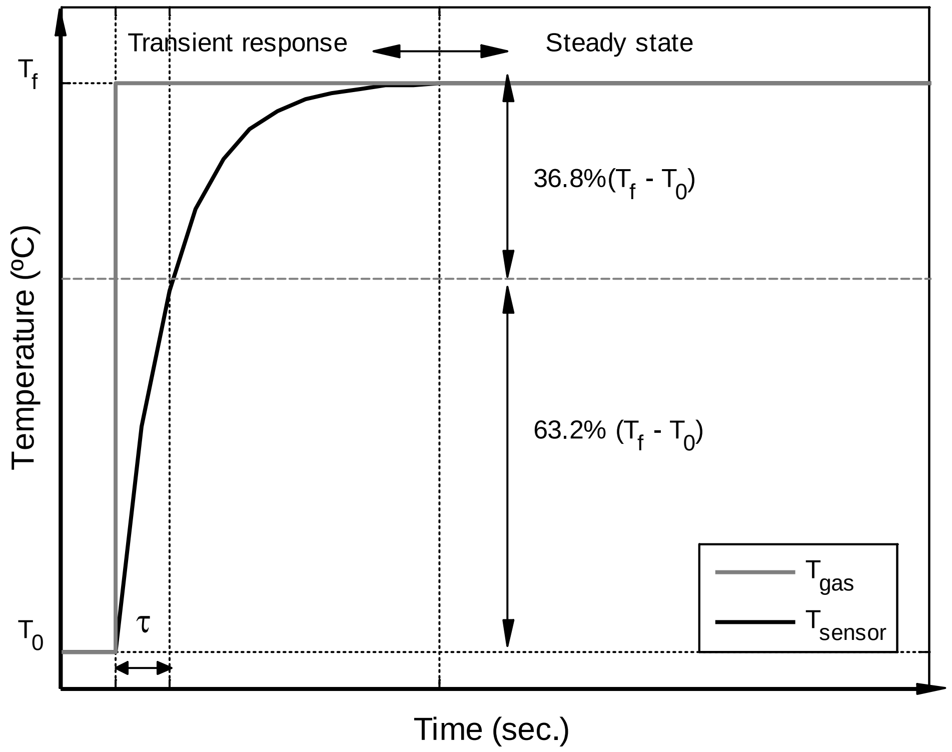

Figure 2 Response of a thermocouple to a step change of temperature

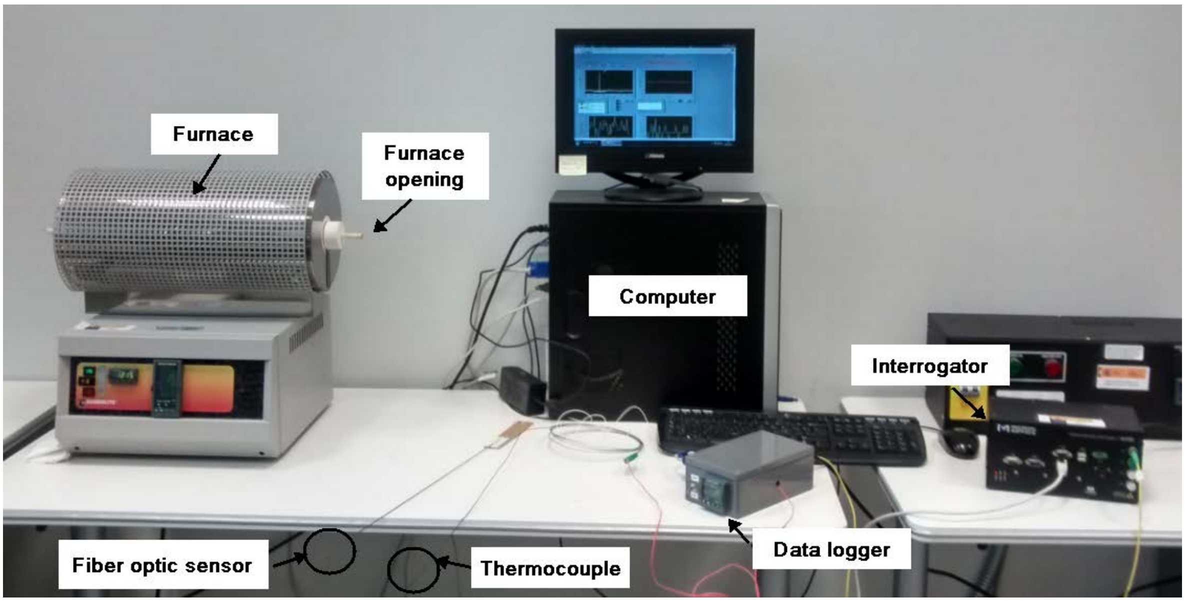

Figure 3 Experimental test layout

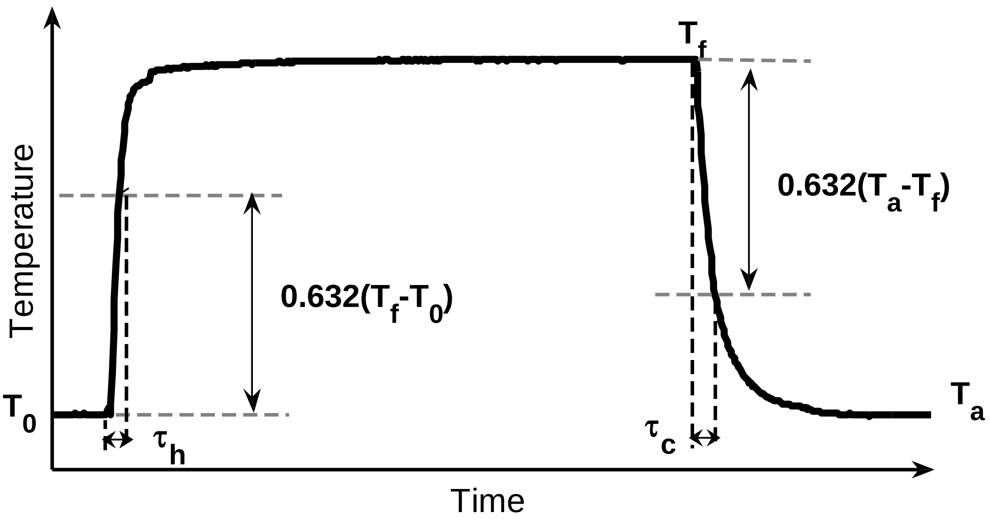

Figure 4 Typical response of a sensor throughout the response time test

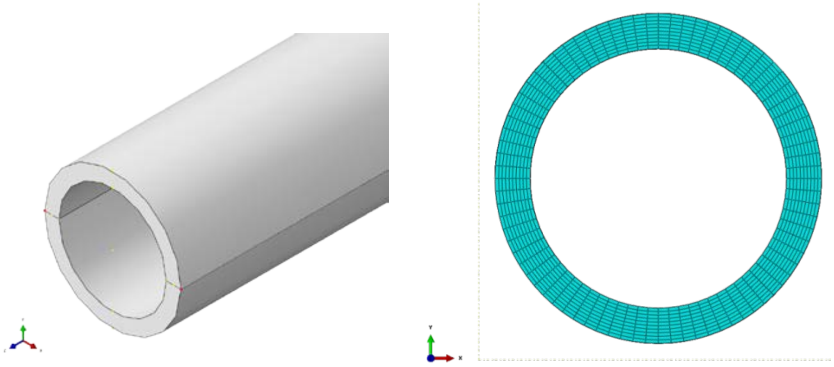

Figure 5 a) Geometry of the non-linear heat transfer model. FOS A, external diameter 1.5 mm and thickness 0.15 mm. 3D view. b) Meshed cross section of the model

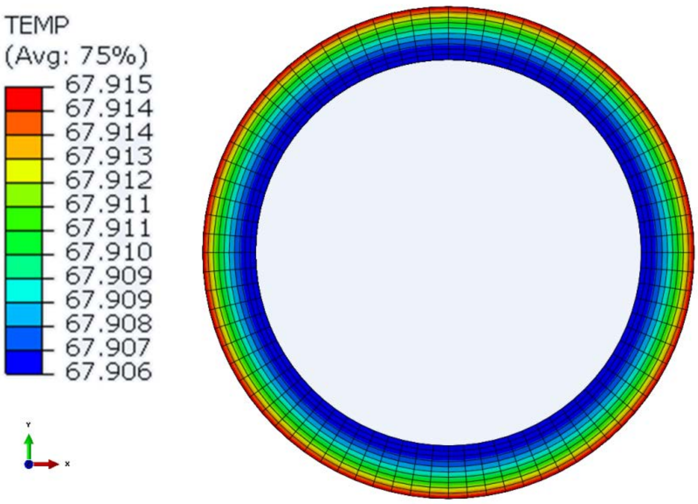

Figure 6. Temperature (°C) along the cross section of the sensor type A. For T_f = 100°C and t=8s

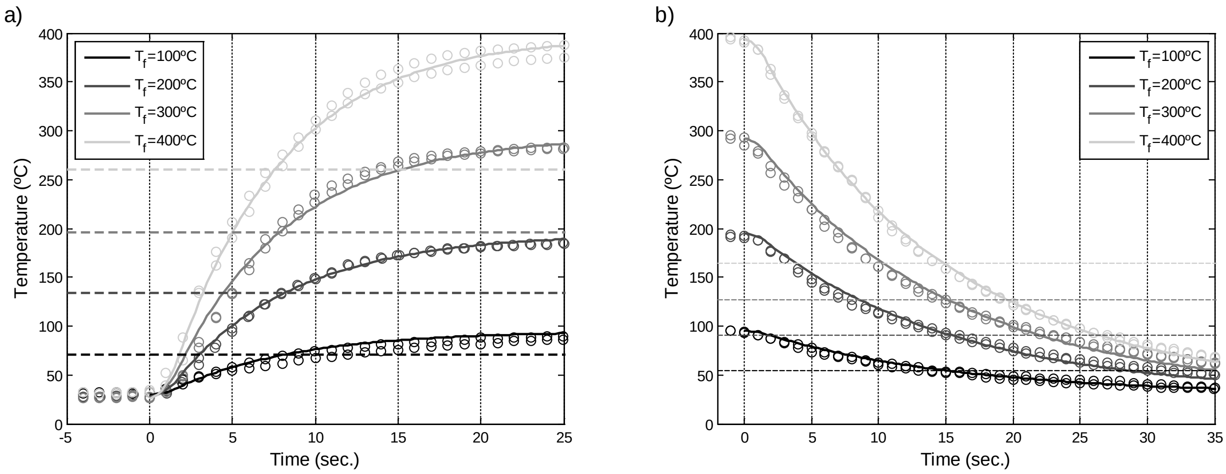

Figure 7 Sensor A. Sensor response with furnace temperatures of 100°C, 200°C, 300°C and 400°C. Continuous lines represent analytical solution. Circles represent experimental results. a) Heating phase; b) Cooling phase.

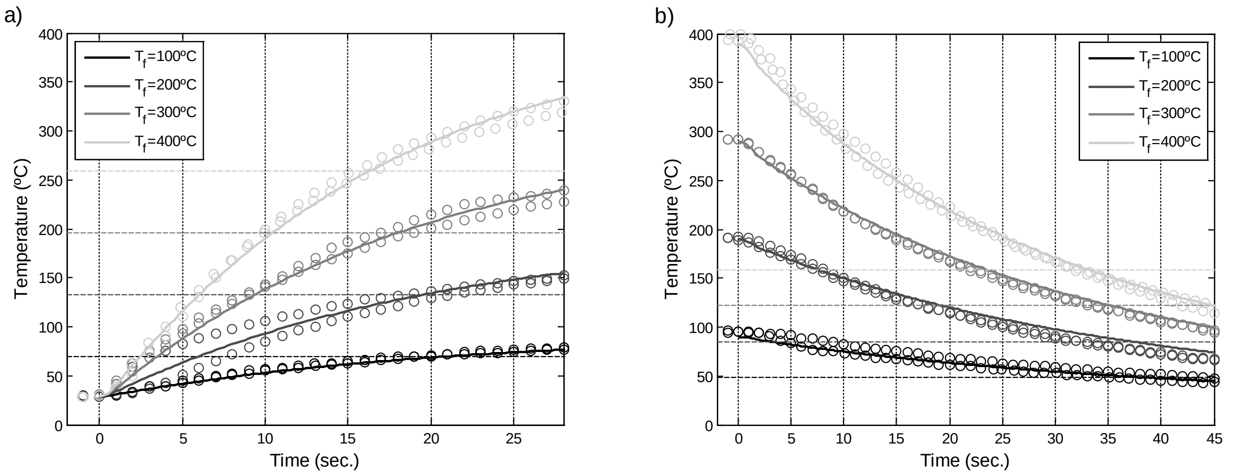

Figure 8 Sensor B. Sensor response with furnace temperatures of 100ºC, 200ºC, 300ºC and 400ºC. Continuous lines represent analytical solution. Circles represent experimental results. a) Heating Phase; b) Cooling phase.

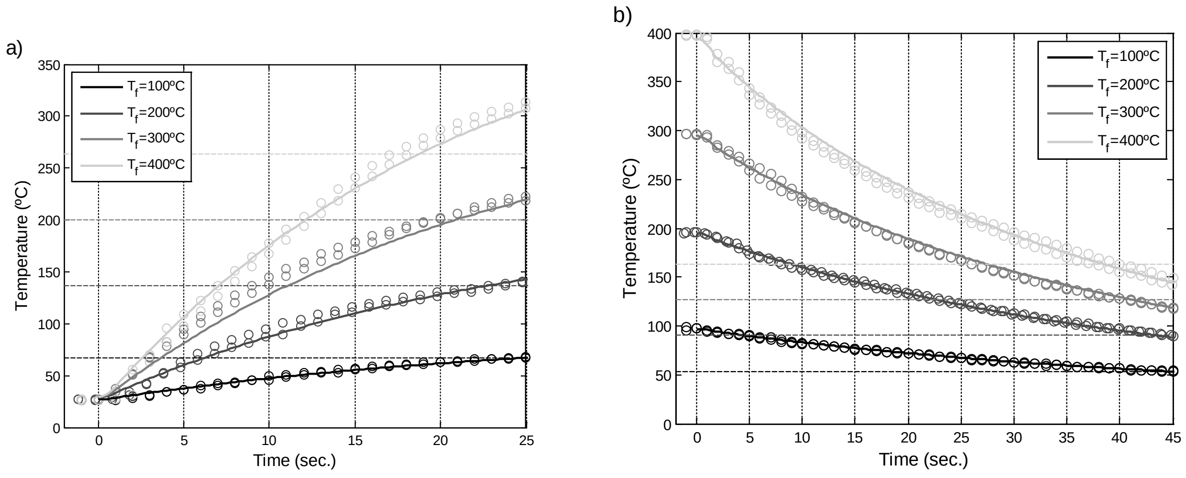

Figure 9 Sensor C. Sensor response with furnace temperatures of 100ºC, 200ºC, 300ºC and 400ºC. Continuous lines represent analytical solution. Circles represent experimental results. a) Heating Phase; b) Cooling phase.

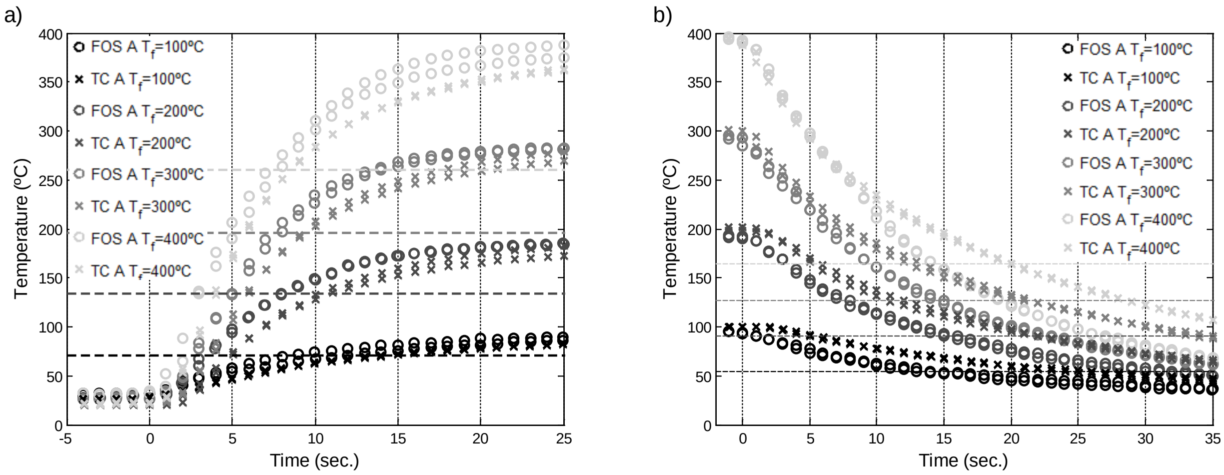

Figure 10 Comparison of the dynamic response of Fiber Optic Sensor A (FOS A, circles) and Thermocouple A (TC A, x) with furnace temperatures of 100°C, 200°C, 300°C and 400°C. a) Heating Phase; b) Cooling phase.

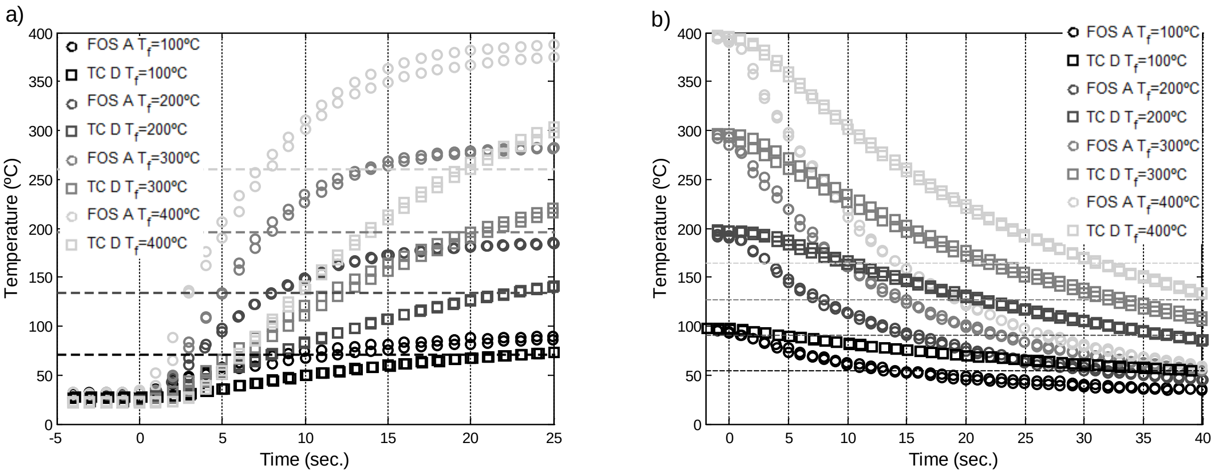

Figure 11 Comparison of the dynamic response of Fiber Optic Sensor A (FOS A, circles) and Thermocouple D (TC D, squares) with Furnace temperatures of 100ºC, 200ºC, 300ºC and 400ºC. a) Heating Phase; b) Cooling phase.

Table 1 Analytical Response times [s] of FOS A, FOS B and FOS C for both heating and cooling phase.

T_f[°C]	Heating phase (τ_h)			Cooling phase (τ_c)		
	FOS A	FOS B	FOS C	FOS A	FOS B	FOS C
100	8.2	20.2	24.2	15.4	38.7	46.0
200	8.1	18.9	22.5	15.4	37.0	43.7
300	7.9	17.3	20.4	15.2	35.0	41.1
400	7.5	15.5	18.1	14.9	32.9	38.3
500	7.1	13.7	15.8	14.4	30.6	35.5
600	6.7	11.8	13.5	13.8	28.3	32.7
700	6.2	10.0	11.4	13.2	26.1	29.9
800	5.7	8.4	9.5	12.5	24.0	27.3
900	5.3	7.0	7.8	11.8	22.0	24.9
1000	4.8	5.7	6.4	11.1	20.1	22.6
1100	-	7.6	5.2	-	18.3	20.6
1200	-	3.6	-	-	16.7	18.7

Table 2 Experimental Response times [s] of TC A, TC D and FOS A for both heating and cooling phases for furnace temperatures of 100°C, 200°C, 300°C and 400°C.

T_f [°C]	Heating phase (τ_h)			Cooling phase (τ_c)		
	TC A	TC D	FOS A	TC A	TC D	FOS A
100	13.0	22.0	8.4	24.0	37.1	15.4
200	10.1	21.9	8.1	20.5	35.6	15.4
300	9.2	20.9	7.8	20.0	32.0	15.2
400	8.7	20.0	7.4	19.4	31.0	14.6